

Article

Risk Assessment of World Corn Salinization Hazard Factors Based on EPIC Model and Information Diffusion

Degen Lin ^{1,*} , Chuanqi Hu ², Fang Lian ³ , Jing'ai Wang ^{4,5,6,7,*}, Xingli Gu ⁸ and Yingxian Yu ¹¹ School of Business, Wenzhou University, Wenzhou 325000, China; 21450101023@stu.wzu.edu.cn² Northwest Institute of Historical Environment and Socio-Economic Development, Shaanxi Normal University, Xi'an 710119, China; hcq0917@snnu.edu.cn³ Integrated Research on Disaster Risk (IRDR) International Programme Office, Beijing 100094, China; fang.lian@irdrinternational.org⁴ Faculty of Geographical Science, Beijing Normal University, Beijing 100875, China⁵ Key Laboratory of Environmental Change and Natural Disaster, Ministry of Education, Beijing Normal University, Beijing 100875, China⁶ State Key Laboratory of Earth Surface Processes and Resource Ecology, Beijing Normal University, Beijing 100875, China⁷ Academy of Plateau Science Sustainability, The People's Government of Qinghai Province and Beijing Normal University, Xining 810016, China⁸ College of Geography and Environmental Sciences, Zhejiang Normal University, Jinhua 321004, China; xinligu@zjnu.edu.cn

* Correspondence: 20200661@wzu.edu.cn (D.L.); jwang@bnu.edu.cn (J.W.)

Abstract: Salinization is a serious land degradation phenomenon. This study identified the salinity stress threshold as a causal factor for salinization, focusing on global maize fields as the study area. By excluding environmental stressors and setting salinization scenarios, the EPIC model was used to simulate the daily salinity stress threshold during the corn growth process. The global intensity and risk of salinization-induced disaster for maize were evaluated. Based on the principle of information diffusion, the intensity of salinization-induced disaster was calculated for different return periods. The main conclusions were as follows: (1) By excluding environmental stress factors and setting salinization scenarios, algorithms for the salinization index during the growing season and the intensity of salinization-induced disaster were proposed. (2) The salinity hazard factor is highly risky and concentrated in arid and semi-arid regions, while it is relatively low in humid regions. (3) As the recurrence period increases, the risk of salinization-induced hazard becomes higher, the affected area expands, and the risk level increases. (4) The salinization intensity results of this study are consistent with the research results of HWSO ($R^2 = 0.9546$) and GLASOD ($R^2 = 0.9162$).

Keywords: information diffusion; risk of hazard factor; salt stress; EPIC model



Citation: Lin, D.; Hu, C.; Lian, F.; Wang, J.; Gu, X.; Yu, Y. Risk Assessment of World Corn Salinization Hazard Factors Based on EPIC Model and Information Diffusion. *Land* **2023**, *12*, 2076. <https://doi.org/10.3390/land12112076>

Academic Editors: Mario Al Sayah, Rita Der Sarkissian and Rachid Nedjari

Received: 24 September 2023

Revised: 5 November 2023

Accepted: 10 November 2023

Published: 18 November 2023



Copyright: © 2023 by the authors. Licensee MDPI, Basel, Switzerland. This article is an open access article distributed under the terms and conditions of the Creative Commons Attribution (CC BY) license (<https://creativecommons.org/licenses/by/4.0/>).

1. Introduction

With the advent of the “Anthropocene”, land systems increasingly face complex challenges [1,2], salinization being a prime example requiring human attention. Soil salinization, a severe land degradation phenomenon, arises from the buildup of soluble salts in both the soil cultivation and surface layers [3]. Salinization undermines land productivity, diminishing agricultural output in irrigation areas and impeding agricultural development and food production [4]. Over a hundred countries and regions around the globe deal with varying levels of saline soils. According to data from the United Nations Educational, Scientific and Cultural Organization (UNESCO, Paris, France) and the Food and Agriculture Organization (FAO, Rome, Italy) of the United Nations, the total area of saline soils is around 954.38 million hectares. Salinization poses a significant agricultural risk (risk = hazard factors × exposure × vulnerability) [5]. In some timeframes and regions,

exposure remains relatively steady, with the hazard severity typically determining the risk magnitude. Consequently, several scholars concentrate on the salinization hazards [6–8].

Despite decades of research, comprehensive, large-scale land salinization assessments remain an enduring challenge [9]. Numerous studies concur that obtaining accurate measures of salinization at large scales is a complex task [10–13]. When assessing hazards contributing to salinization, scholars typically select salinization-specific indicators for a comprehensive evaluation, such as cation exchange rate (ECe), average annual evapotranspiration volume, groundwater characteristics, and dry humidity [14]. Initially, the soil's conductivity is usually identified by the ECe of the saturated paste extraction [15–18]. Most studies employ ECe as an index to gauge soil salinization, considering soils with ECe exceeding 4 dsm^{-1} as saline. Secondly, elevated evapotranspiration intensifies water-salt movements, increasing the salt concentration in soil water and on the surface [19,20]. Consequently, the average annual evapotranspiration volume serves as a significant index for assessing salinization risk. Thirdly, groundwater impacts on salinization manifest in two ways: i the depth of the water table, where shallow, semi-closed aquifers can trigger salinization by impeding surface soil drainage [21]; and ii groundwater mineralization, linked to irrigation, as the quality of groundwater used for irrigation influences soil texture. Long-term unsuitable irrigation increases salinization risk [22]. Data acquisition limitations and model parameter validity concerns lead some investigators to select alternate indicators for assessing salinization risk. Some base their evaluation on the depth of the saline soil and the groundwater table [23], others incorporate soil and climate attributes, irrigation water properties, conductivity, cation exchange rate, and dry humidity [14].

Additionally, many scholars have used models to assess the hazards of salinization factors. Currently, the models primarily used to evaluate salinization risk include UN-SATCHEM [24], SALTMED [25], BUDGET [26], Pla [27], and Riverside [18], among others. The first three are complex models, requiring large amounts of data, suitable for assessing small-scale areas, such as farmland and small watersheds, while Pla [19] and Riverside [18] are simpler models, suitable for larger-scale areas, such as farms and large river basins. It is noteworthy that many new methods have emerged in recent years. For instance, Hassani and others utilized machine learning algorithms to make long-term predictions on global salinization issues based on $EC'e''$ [28]; FAO constructed The Global Map of Salt-Affected Soils (GSASmap) platform based on indices like $EC'e$, ESP, PH [29]; Kaya and others adopted remote sensing methods to assess soil salinization conditions in the western part of Turkey based on $EC'e''$ [30].

Contemporary research frequently employs external factors such as soil characteristics, climate variability, and groundwater dynamics as metrics to assess the hazards of soil salinization to agricultural productivity. Nonetheless, these indicators may inadvertently sidestep the direct effects of salinization on the crops themselves, potentially obscuring the isolated impact of saline conditions on plant growth. Addressing this gap, our study proposes the utilization of normalized salt stress values, correlated to the crop growth cycle, as a more precise measure of salinization impact, thereby elucidating the independent extent of salt-induced stress on crop vitality. The EPIC crop growth model, known for its robustness, is employed to establish salinization scenarios, which delineates the day-to-day susceptibility of crops to saline disturbances. The selection of crop species is pivotal for the applicability of such growth models. Maize, with its global significance as a staple crop [31], wide cultivation range [32], and intermediate salinity tolerance [33], represents an ideal candidate for this analysis. This research focuses on global cornfields, uses the EPIC0509 model to simulate the salinity stress value [34–37] during corn growth with days as steps, attempts to evaluate the risk of salinization hazard intensity about corn on a global scale, and calculates the salinization hazard intensity under different recurrence periods based on the principle of information diffusion [38].

2. Materials and Methods

2.1. Basic Concepts and Research Framework

2.1.1. The EPIC Crop Growth Model

The erosion-productivity impact calculator (EPIC) model was developed in 1981 by Williams et al. to study the relationship between soil erosion and soil productivity [39–41]. Initially, the value of the EPIC model in simulating crop growth was not noticed. It was not until 1989 that the EPIC model began to be used as a crop growth model [42]. In 1996, Williams et al. incorporated environmental factors such as water quality, carbon cycle, and climate change into the EPIC model, subsequently renaming it the “Environmental Policy Impact Climate” model [43]. Due to the EPIC model’s ability to simulate crop productivity over hundreds or even thousands of years in various climate scenarios, environmental conditions, and management systems, assessing the impact of multiple agricultural disasters on crop yield and land productivity, it has become one of the most popular crop growth models [44–46]. Some studies even suggest that, in terms of model calibration and crop yield evaluation, the EPIC model performs better than the CSM-CERES-Maize [47].

2.1.2. Mechanism of Salt Stress in Maize

Salinity stress affects almost all crucial metabolic processes of corn growth [48]. Based on previous research, the damaging mechanisms of salinity stress on corn mainly include the following aspects: (1) Salinity stress leads to difficulties in corn water absorption. Due to the high salt content in saline soils, the soil solution water potential significantly decreases, causing difficulties in water absorption of corn roots, or they cannot absorb water at all. In severe cases, it even leads to the outward discharge of water, causing osmotic dehydration of the tissue and harming corn [49,50]. (2) Salinity stress has detrimental effects on the corn biomembrane. Studies indicate that the membrane plays a crucial role in generating primary and secondary stress responses. Salt stress influences various aspects of membrane function, including ion selective permeability, transport of inorganic and organic matter, membrane secretion function, membrane lipid composition, and ultrastructure [51–53]. (3) Salinity stress causes physiological disorders in corn. Salinity stress affects the physiological activities of corn, for instance, salt stress causes a decline in the net photosynthesis rate of corn [54–56], and salinity stress disrupts normal respiratory metabolism and protein synthesis of corn [57–59].

2.1.3. Hazard Intensity Assessment and Information Diffusion Method

The core of the disaster factor hazard assessment is to establish a relationship between the disaster intensity and frequency. The hazard assessment of disaster-inducing factors can be divided into the average expected disaster intensity and the probability that the intensity of the disaster factor exceeds a certain value (the frequency of the disaster factor) [60]. Calculating the frequency of disaster factors requires a large amount of sample data. However, when the sample information is incomplete, the information diffusion method can be used to calculate the frequency of disaster factors, and a fuzzy set is obtained after diffusing the original incomplete information. This is a method of treating samples collectively using fuzzy mathematical methods to compensate for information deficiencies [61]. Specifically, using the diffusion function to convert sample data into sample sets, the simplest model is the normal diffusion model [38]. This paper calculates the intensity of disaster factors with different probabilities of occurrence (recurrence periods of 10, 20, 50, 100 years) by diffusing the salinization hazard factors of the 30-year samples through information diffusion.

2.1.4. Research Framework

This study is conducted in four steps. The first step is to establish the database. The second step is to determine the hazard-inducing factor-salt stress and eliminate other environmental stress factors. The third step is to simulate the growth process of corn using the EPIC model and, based on the daily salt stress value, calculate the index of salinization hazard intensity. The results are then compared with existing salinization results (HWS

and GLASOD). The fourth step, based on the principle of information diffusion, is to calculate the hazard intensity of corn salinization under the recurrent periods of 10 years, 20 years, 50 years, and 100 years (Figure 1).

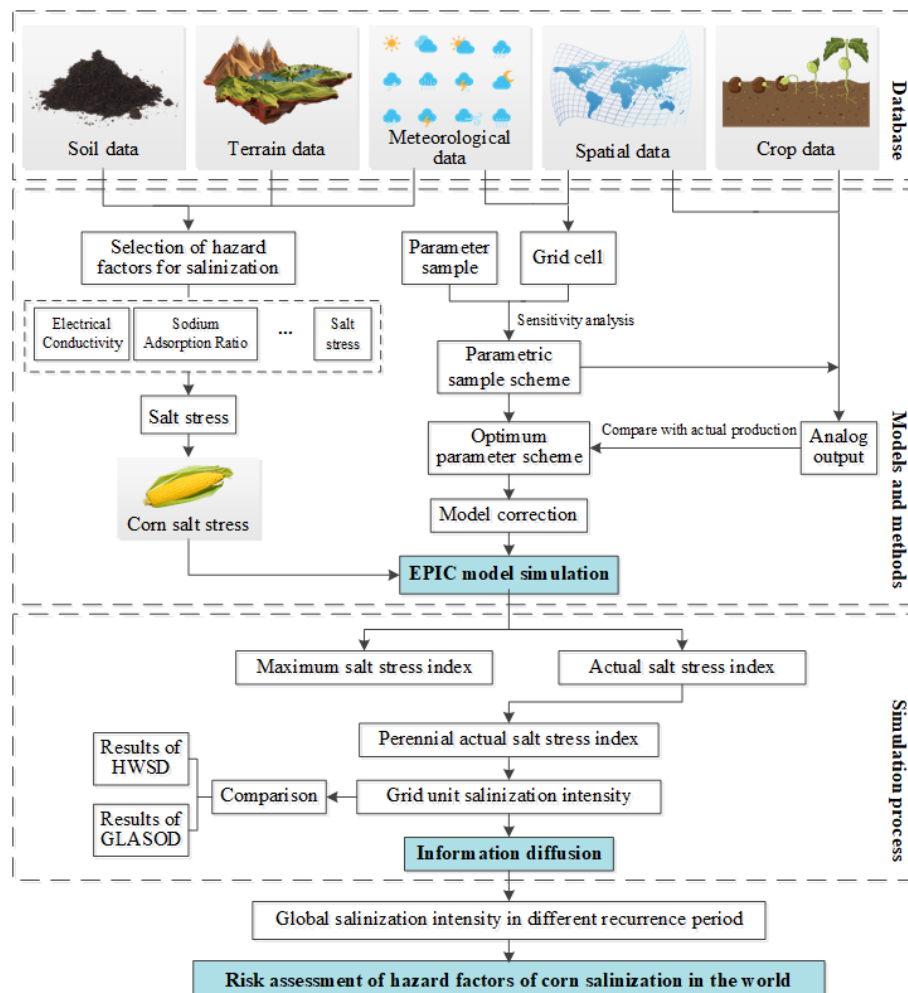


Figure 1. The research framework.

2.2. Data

Based on the research approach, this paper uses the EPIC0509 model to calculate the hazard intensity of salinization. In the research, a data list required was constructed, as shown in Table 1.

Table 1. Datasets for world corn salinization.

Data Name	Data Content	Spatial Resolution	Temporal Resolution	Data Sources
DEM	Global elevation	0.0833° × 0.0833°	1997	USGS [62]
Slope	Global slope	0.0833° × 0.0833°	1997	GAEZ [63]
Soil Properties	Global soil distribution raster image and soil physical and chemical properties such as PH, soil depth, conductivity, etc.	0.0833° × 0.0833°	1995	ISRIC

Table 1. Cont.

Data Name	Data Content	Spatial Resolution	Temporal Resolution	Data Sources
Meteorological	Global precipitation, temperature, solar radiation, and other information	0.5° × 0.5°	1971–2099	Cross-sector impact model comparison projectRCP2.6 [64]
Planting Area	Global cultivation crop region	5 min × 5 min	1992	Sustainability and the Global Environment, University of Wisconsin-Madison [65]
Corn Parameter Data	Corn EPIC Model Reference (US)	Site	-	Texas A&M University College of Agriculture and Life Sciences
Growth Period	Corn planting time and growth period length	0.5° × 0.5°	2000–2015	Nelson Institute for Environmental Studies at the University of Wisconsin-Madison [66]
Irrigation	Global annual irrigation water of agriculture(mm)	0.5° × 0.5°	1995	Institute of Industrial Science, University of Tokyo [67]
Fertilizer	Global annual fertilizer application for maize	0.5° × 0.5°	2012	Earth stat [68]
Corn production	Production data for global country units	Vector unit	1995–2004	FAO
	China provincial unit production data	Vector unit	1995–2004	Department of Plantation Management, Ministry of Agriculture, China
	US state unit production data	Vector unit	1995–2004	United States Department Of Agriculture
	Australian state unit production data	Vector unit	1995–2004	Australian Bureau of Statistics
	India state unit production data	Vector unit	1995–2004	Department of Agriculture and Cooperation
Evaluation unit	World administrative divisions, rivers, lakes, etc.	Vector unit	1995–2004	ESRI, China Surveying and Mapping Geographic Information Bureau, CRU TS2.1, DIVA-GIS
Aridity Index	Global Map of Aridity	10 arc minutes	1961–1990	FAO [69]
Other salinization research results	Excess salts	0.5° × 0.5°	1971–1981	Harmonized World Soil Database [70]
	Cs	Vector unit	1991	GLASOD [71]

2.3. Method

2.3.1. Features and Simulation Process of EPIC0509

The version of the EPIC model used in this study is EPIC0509, which is a classic version officially developed by EPIC and released in 2006 [34]. This version has the following features: It operates on a daily timestep, capable of simulating crop growth conditions

for 1–4000 years; the model provides basic soil, weather, tillage, and crop parameters; the soil can be divided into 10 layers; there is an optional weather generator; and the site-specific model has been improved to a field-scale model. It is widely used in crop growth simulation [28,72–74]. The main simulation process of the EPIC0509 model can be divided into 4 steps (Figure 2): (1) based on temperature (temperature and heat required by crops) to simulate the phenological development of crops, with heat unit index as the characterization index, this process affects the calculation of leaf area and root weight; (2) the growth of potential biomass of crops was simulated based on light energy (solar radiation, sunshine hours and light energy conversion rate), with leaf area index as the core index; (3) simulated the environmental stress (water, salt, temperature and nutrients) during the growth of crops. Among them, the maximum stress value was involved in the simulation calculation of leaf area and aboveground biomass; and (4) simulated crop yield based on aboveground biomass and harvest index, in which aboveground biomass was comprehensively affected by root weight, potential biomass, and environmental stress, and harvest index was affected by environmental stress and potential harvest index.

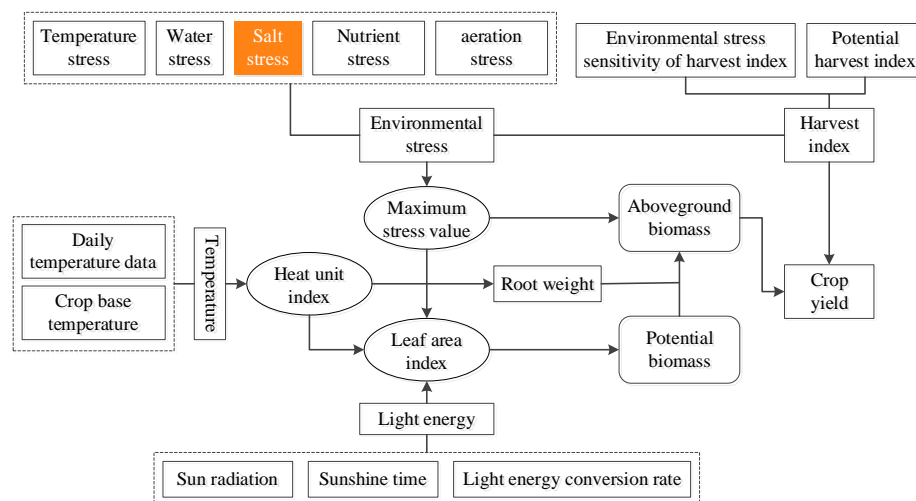


Figure 2. EPIC crop growth model simulation process.

2.3.2. Identifying Hazard Factors for Corn Salinization

In the previous experimental studies on the effects of salinization on crops, the evaluation was generally based on soil salinity combined with certain environmental conditions to construct hazard indicators, which cannot accurately reflect the independent impact of salinity on crops. The EPIC model simulates various environmental stress values in the crop growth process on a daily basis, which reflect the independent severity of different stresses on crop growth. The salinity stress value is calculated based on the crop's irrigation conditions and original soil conditions, and it quantifies the yield loss caused by the final soil salinity concentration.

Soil salinity is closely related to irrigation, and its calculation formula is as follows [42]:

$$WSLT_{i+1} = WSLT_i + 0.01 \times AIR_i \times CSLT_i \quad (1)$$

WSLT: Soil salinity content; *AIR*: maximum irrigation amount per time; *CSLT*: salt concentration in irrigation water.

Soil moisture content has a significant impact on soil salinity stress, and its calculation formula is as follows [42]:

$$ST_{i+1} = ST_i + AIR_i \quad (2)$$

ST: Soil moisture content; *AIR*: maximum irrigation amount per time.

The daily salt stress value is the hazard factor of this study, and its calculation formula is as follows [42]:

$$SWRZ_{i+1} = SWRZ_i + ST_i \times (RZ - Z_{i-1}) / (Z_{i-1} - Z_i) \quad (3)$$

$$TSRZ_{i+1} = TSRZ_i + WSLT_i \times (RZ - Z_{i-1}) / (Z_{i-1} - Z_i) \quad (4)$$

$$SS = a \times (0.15625 \times TSRZ / SWRZ - b) \quad (5)$$

SS: The daily salinity stress value. In addition, $SWRZ$ and $TSRZ$ are the intermediate variable, the initial value is 0.

The calculation formula for salinity stress during the maize growth period is as follows [75]:

$$SS_{Total} = \sum_{i=1}^{total} SS_i \quad (6)$$

SS_{Total} represents the total salinity stress value during the maize growth period, and SS_i represents the salinity stress value for the i -th day.

2.3.3. Intensity of Hazard Caused by Corn Salinization

Constructing an index for the intensity of salinization hazard based on daily salinity stress values [75].

$$SI = \frac{SS_{total}^i}{\max(SS_{total}^i)} \quad (7)$$

Among them, SS_{total}^i : total salt stress in the scenario i , $\max(SS_{total}^i)$: the largest total salt stress value of scenarios in the current year.

The maximum value of salinity stress in a given year is obtained through the simulation of salinization scenarios. In the EPIC model simulation, there are three main aspects that can cause yield reduction in crops, and corresponding measures are taken to mitigate them. First, field management measures, including diseases, pests, and management errors, are automatically excluded in the simulation. Second, soil erosion conditions, such as water erosion and wind erosion, are eliminated by disabling the water erosion and wind erosion modules in the model, thus not considering their influence during the simulation. Third, environmental stress factors, including temperature stress, nutrient stress (nitrogen, phosphorus, potassium), water stress, and ventilation stress, are addressed by setting appropriate parameters in the model to exclude these environmental stress factors (Table 2).

Table 2. Elimination of environmental stress elements.

Elimination of Coercion Type	Elimination Method
Temperature stress	Management measures automatic fertilization
Nutrient stress	Management measures automatic fertilization
Water stress	Set up automatic irrigation to meet crop water requirements
Ventilation stress	Pre-experiment setting the maximum water supply so that no ventilation stress is generated

According to the calculation formula of the salinity stress value, it can be inferred that salinity is involved in the hazard process of salinization through the initial soil salinity and irrigation water salinity, while the final soil salinity content affects crop yield. Therefore, in the model simulation process of the scenarios with the highest total salt stress, we set the initial soil salt concentration, namely conductivity, as 0, and established the highest salt concentration of irrigation water to obtain the extreme yield loss scenario.

2.3.4. Calculation of Crop Yield

The salt tolerance of crops to salinization is closely related to their species and variety [76]. The classification criteria for determining the salt tolerance of crops are based on soil salinity, evapotranspiration loss, and water daily stress index. The calculation formulas for crop yield under salt stress caused by different dominant factors vary [77]. In cases where the dominant factor of salt stress is soil salinity, the crop yield formula is as follows:

$$Y = 100 - b(EC_e - a) \quad (8)$$

Y is relative yield, EC_e is the electrical conductivity of soil solution (dS/m), a is the threshold electrical conductivity tolerance of the crop (dS/m), and b is the slope, which represents the reduction rate of yield per unit electrical conductivity.

2.3.5. Salinization Hazard Intensity Recurrence Algorithm

Information diffusion is a method based on fuzzy set theory for comprehensive evaluation of regional environmental risks [78]. Its specific application in this study is as follows:

The indices of salinization hazard intensity are statistically analyzed, with these hazard intensity indices denoted as x_1, x_2, \dots, x_m , then

$$X = \{x_1, x_2, \dots, x_m\} \quad (9)$$

X is the observation sample set, x_i is the index of the hazard intensity caused by salinization of a cornfield in the i th year ($i = 1, 2, \dots, m; m = 24$);

Let the domain of the hazard intensity index be U :

$$U = \{u_1, u_2, \dots, u_n\} \quad (10)$$

Each individual data sample, denoted as x_i , can diffuse the information it carries to all points in the domain of hazard intensity index U using Formula (10):

$$f_i(u_j) = \frac{1}{h\sqrt{2\pi}} \exp\left[-\frac{(x_i - u_j)^2}{2h^2}\right] \quad (11)$$

The variable h is referred to as the diffusion coefficient, and its value can be determined based on the maximum and minimum values of the hazard intensity index in the sample set, as well as the number of samples m . The calculation formula for h is as follows:

$$h = 2.6851(b - a)/(m - 1) \quad (12)$$

where $a = \min_{1 \leq i \leq m} \{x_i\}$, $b = \max_{1 \leq i \leq m} \{x_i\}$.

Based on this value, an estimation of the hazard intensity beyond the probability can be obtained [2].

3. Results

3.1. Mean Expected Hazard Intensity of Global Corn Salinisation

In this study, meteorological station data from 1971 to 2004 were selected. The actual conductivity content in the soil was used as a substitute for irrigation water salinity to calculate the salinization index (SI) for each year and grid in the 0.5×0.5 grid unit. The expected results of salinization hazard intensity were obtained and presented in Figure 3.

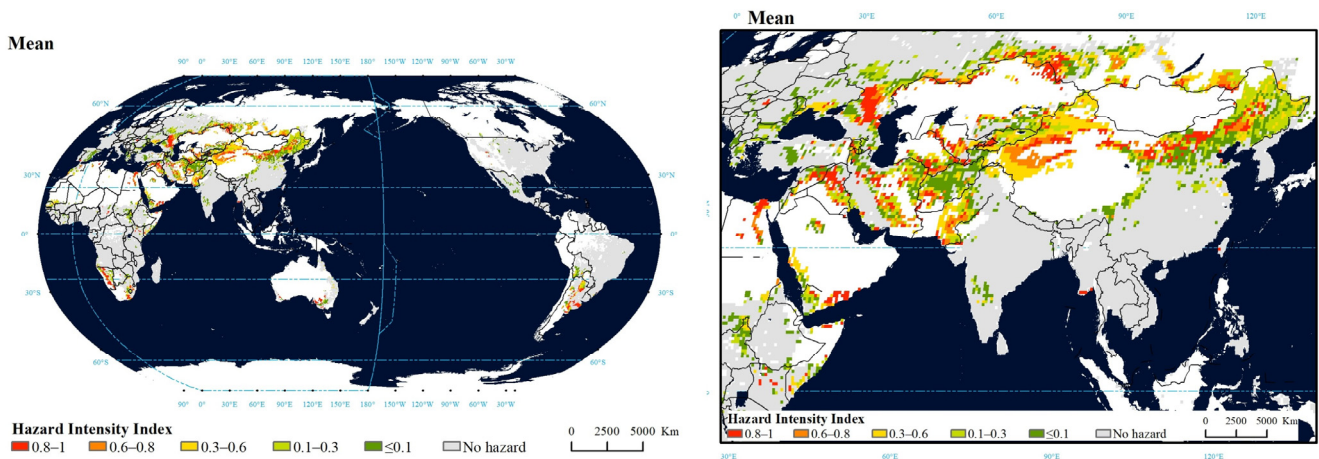


Figure 3. Mean expected hazard intensity of global corn salinization.

According to Figure 3, the red areas in the graph (with hazard index > 0.8) indicate the highest salinization hazard intensity for maize. These areas are primarily distributed in Central Asia, northwestern China, southern South America, and the western coast of southern Africa. Asia is identified as the region facing the most severe salinization threat. Oman, the southern part of the high mountains and basins in northwestern China, the plains and hills in central-western Kazakhstan, and the mountainous regions in the northeastern plains all have an average salinization hazard index above 0.5. Additionally, the Nile River Delta and the western side of the South African plateau, as well as the central-northern plateau in Algeria, are also high-risk areas for salinization.

The salinization hazard intensity is related to aridity levels [79]. Based on the aridity classification data from the FAO Global Map of Aridity, the salinization hazard intensity is correlated with the aridity level. Subsequently, the salinization data are categorized based on the aridity level to study the distribution of salinization grid points in each category (Figure 4).

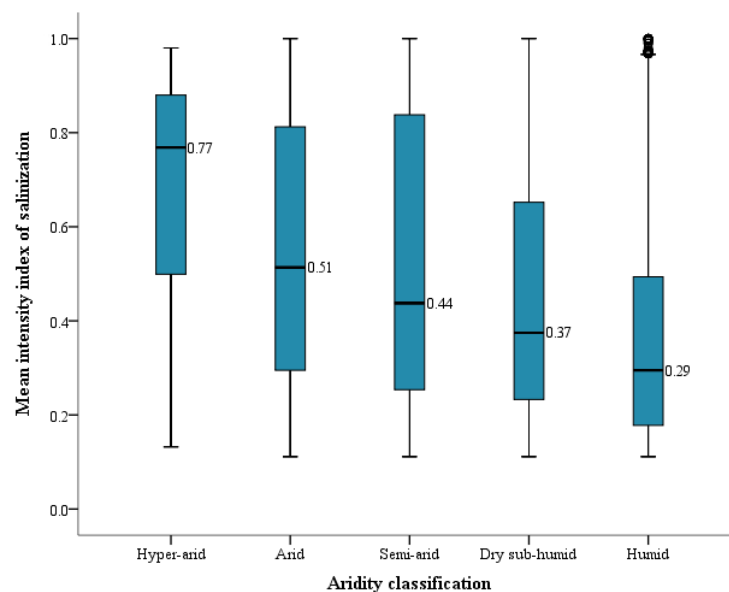


Figure 4. Boxplots of salinization index for different aridity types.

According to Figure 4, the salinization hazard intensity index is highest in hyper-arid regions, with a median value of 0.77 and an interquartile range of approximately 0.4, indicating a relatively high and concentrated salinization intensity in that area. Arid and semi-arid regions also exhibit high salinization hazard intensity, with median values of

0.51 and 0.44, respectively, and interquartile ranges of 0.5 and 0.6, suggesting relatively high salinization intensity but with more dispersed values in these regions. Dry sub-humid regions, as transitional zones between arid and humid areas, show a median salinization hazard intensity index of 0.37, lower than the previous three types, indicating a decrease in salinization intensity. Humid regions have the lowest salinization hazard intensity index, with a median value of 0.29 and an interquartile range of approximately 0.3. The values are concentrated between 0.2 and 0.5, indicating a relatively low and concentrated salinization intensity in that area. Additionally, the boxplot reveals some outliers with higher salinization hazard intensity index in the humid region. This suggests that the salinity index is generally low in Humid, but there are some areas of high salinity along the coast of the sea and inland lakes. In summary, arid and semi-arid regions exhibit higher salinization levels, while humid regions experience relatively lower salinization intensity.

3.2. Global Risk Assessment of Salinization Hazard Factors with Different Return Periods

When sample information is incomplete in the assessment of hazard factor risk, the information diffusion method can be used to calculate the exceedance probability of a certain hazard intensity. In this study, based on the information diffusion model, the salinization hazard factors of a 30-year sample were calculated for different occurrence probabilities (return periods of 10, 20, 50, and 100 years). Figure 5 illustrates the results of salinization hazard intensity calculation. This study also conducted a statistical analysis of the top ten countries in terms of average salinization intensity under different return periods, as shown in Table 3. Additionally, we calculated and ranked the average salinization intensity under different return periods for the top ten largest countries in the world by land area (Table 4).

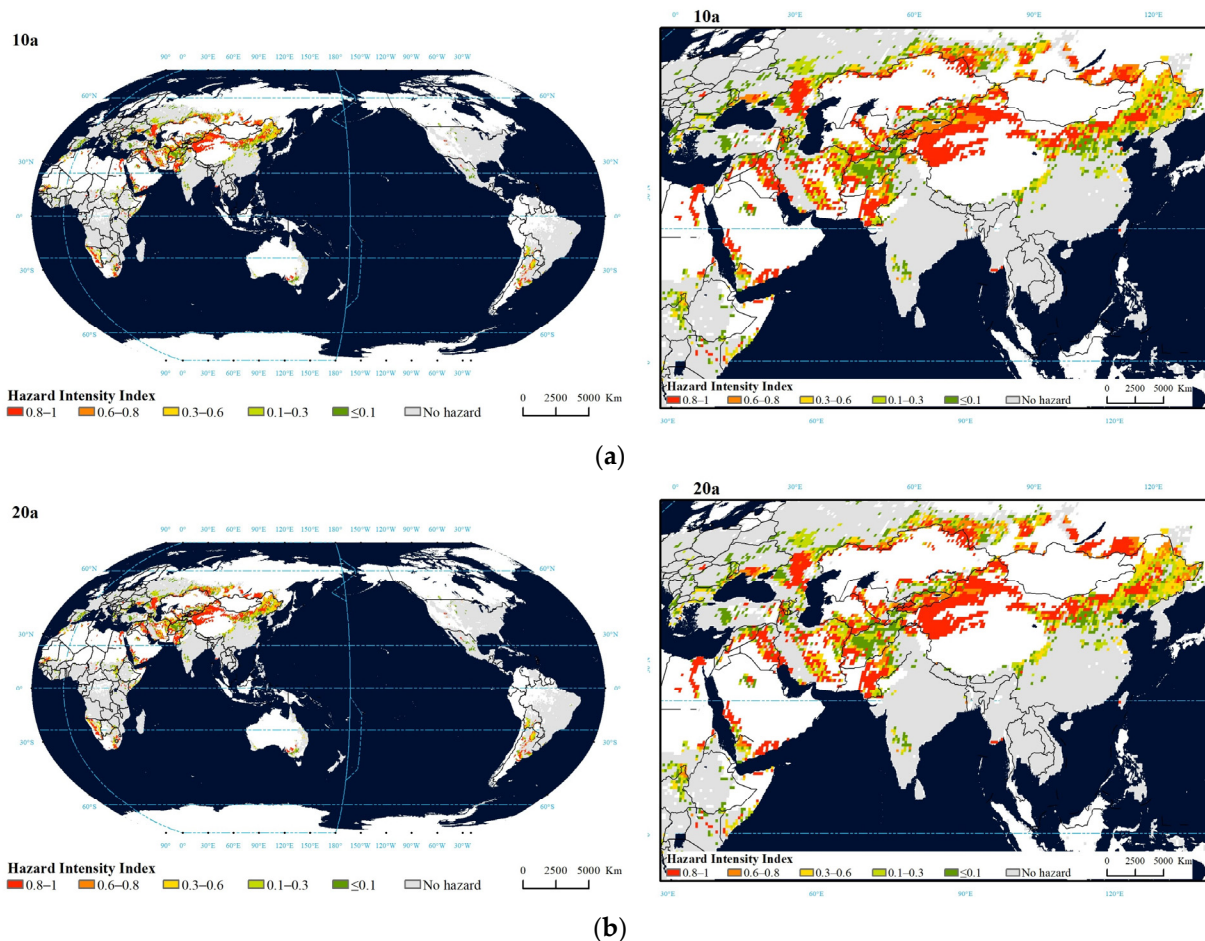


Figure 5. Cont.

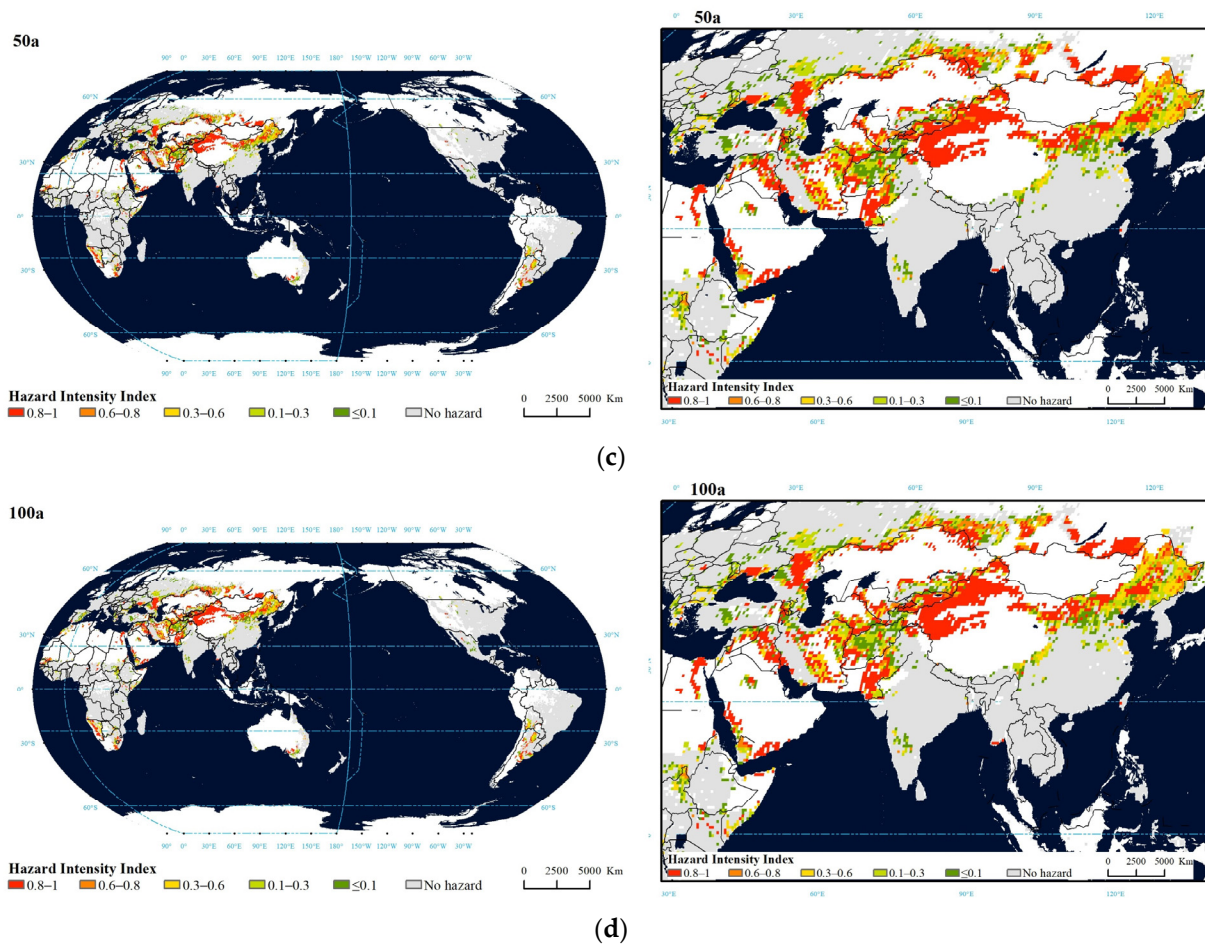


Figure 5. Global salinization hazard intensity under different return periods: (a) 10-year return period; (b) 20-year return period; (c) 50-year return period; (d) 100-year return period.

Table 3. Top ten countries and their average salinization intensity values under different return periods.

Rank	10-Year-Return-Period		20-Year-Return-Period		50-Year-Return-Period		100-Year-Return-Period	
	Country	Mean	Country	Mean	Country	Mean	Country	Mean
1	Oman	0.99	Oman	0.99	Oman	1.00	Oman	1.00
2	Egypt	0.90	Egypt	0.91	Egypt	0.92	Egypt	0.92
3	Mongolia	0.73	Mongolia	0.78	Mongolia	0.82	Mongolia	0.84
4	Kuwait	0.65	Kuwait	0.66	Kuwait	0.66	Kyrgyzstan	0.67
5	Turkmenistan	0.62	Turkmenistan	0.64	Turkmenistan	0.65	Kuwait	0.66
6	Yemen	0.58	Kyrgyzstan	0.61	Kyrgyzstan	0.65	Turkmenistan	0.66
7	Uzbekistan	0.57	Yemen	0.60	Yemen	0.61	Yemen	0.62
8	Kyrgyzstan	0.56	Uzbekistan	0.58	Uzbekistan	0.59	Uzbekistan	0.60
9	Algeria	0.56	Algeria	0.57	Algeria	0.58	Saudi Arabia	0.59
10	Iraq	0.54	Saudi Arabia	0.56	Saudi Arabia	0.58	Algeria	0.58

Table 4. Ranking of the 10 largest countries in terms of average intensity of salinization for different return periods and their average salinization intensity values.

Country	10-Year-Return-Period		20-Year-Return-Period		50-Year-Return-Period		100-Year-Return-Period	
	Rank	Mean	Rank	Mean	Rank	Mean	Rank	Mean
Russia	28	0.19	29	0.20	29	0.20	29	0.21
Canada	68	0.00	68	0.00	69	0.01	69	0.01
China	21	0.30	21	0.31	21	0.32	21	0.33
United States	69	0.00	69	0.00	70	0.00	70	0.00
Brazil	76	0.00	76	0.00	76	0.00	76	0.00
Australia	35	0.09	36	0.09	36	0.10	36	0.10
India	63	0.01	64	0.01	63	0.01	63	0.01
Argentina	27	0.20	27	0.20	28	0.21	28	0.21
Kazakhstan	14	0.45	14	0.46	14	0.47	14	0.48
Algeria	9	0.56	9	0.57	9	0.58	10	0.58

The influence range of high salinization-induced disaster intensity expands with an increase in the return period, as evidenced by Figure 5, Tables 3 and 4. Conversely, the influence range of low salinization-induced disaster intensity decreases. The ranking of total salinization intensity remains relatively stable across different recurrence periods. Specifically, during return periods of 10, 20, 50, and 100 years, Oman, Egypt, and Mongolia consistently ranked in the top three countries worldwide, with an average disaster intensity of over 0.7 (Table 3). However, the rankings of the last seven countries within the top ten for average salinization intensity have shown slight fluctuations. For instance, Kuwait ranked fourth during the 10-year and 20-year return periods, but dropped to fifth during the 100-year return period. Similarly, Kyrgyzstan ranked eighth during the 10-year return period but improved to fourth during the 100-year return period. In terms of the recurrence periods of 10, 20, 50, and 100 years, the rank of mean salinity intensity among the ten countries with the largest areas remained stable (Table 4). Among the countries mentioned, Algeria, Kazakhstan, China, and Russia exhibit relatively high average salinization intensity, ranking 9th, 14th, 21st, and 28th, respectively, worldwide. Remarkably, despite being the smallest among them, Algeria achieves the highest ranking. Algeria consistently experiences an average intensity of salinization greater than 0.5 during the four recurrence periods, placing it around 9th globally. This phenomenon is closely linked to the predominantly dry climate in Algeria's savanna and tropical desert climate zones. In contrast, Brazil, ranking fifth in terms of area, faces comparatively low salinization, with a ranking of 76. This occurrence can be attributed to the majority of Brazil's geographical location in a humid area.

4. Discussion

4.1. Comparison of Salinization Results

4.1.1. Model Validation

We conducted parameter sensitivity analysis, parameter adjustment, and validation on the model using corn yield to ensure the simulation accuracy of the EPIC0509 model. The specific process can be found in the Yin's paper [80–82].

4.1.2. Compared to the Excess Salts Data

In order to evaluate the stability of the research results, we conducted a non-parametric correlation test, specifically the Spearman's rank correlation test, between the results of this study and the excess salts data from the Harmonized World Soil Database v 1.2 (HWSD), at the national and comparable geographical unit scales [60]. The results showed a significant correlation between the two at the 0.01 level. Additionally, the comparison results between the national and comparable geographical units were depicted as scatter plots and data distribution graphs for the salinization levels (as shown in Figure 6).

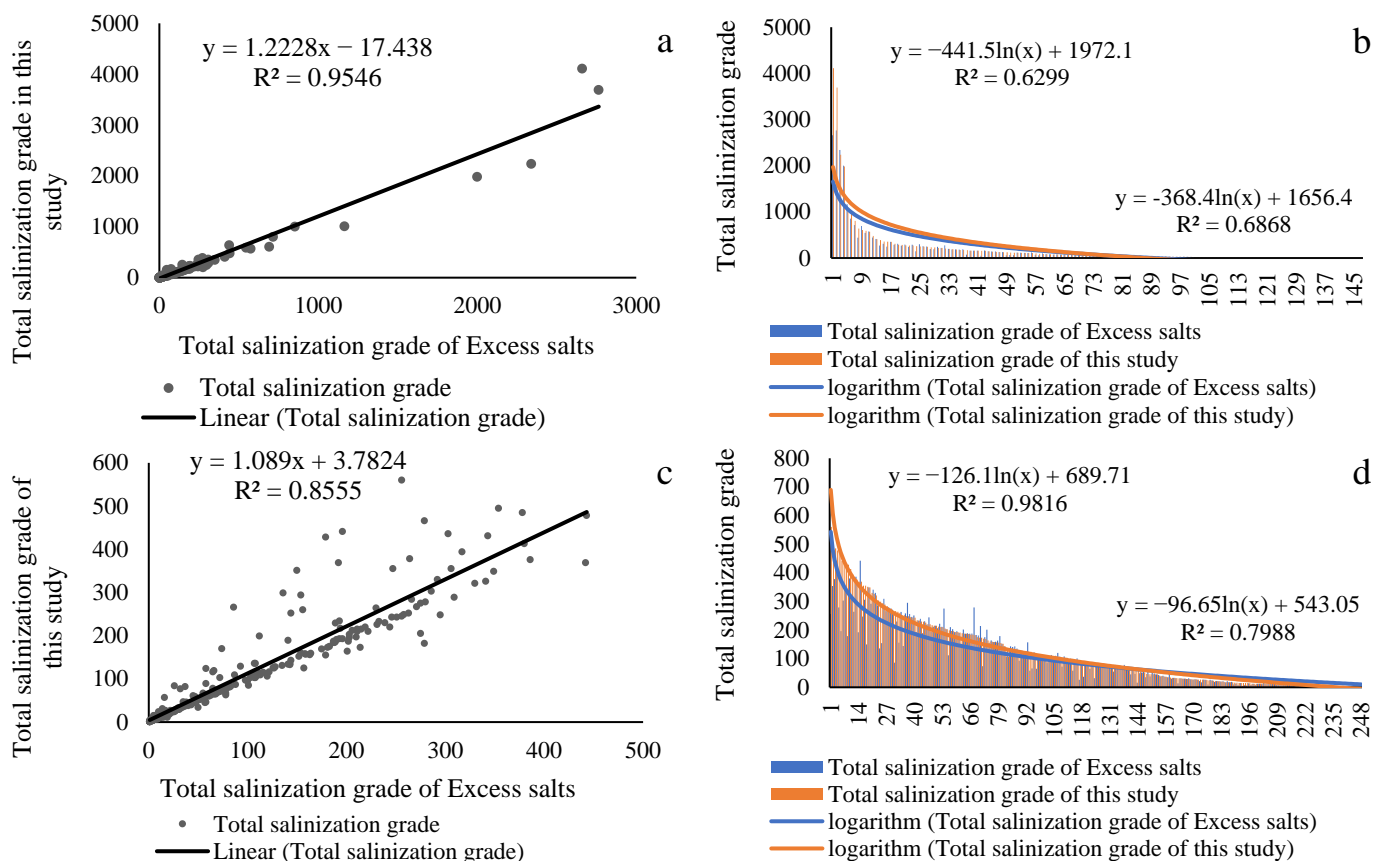


Figure 6. Comparison with Excess Salts at national unit and comparable geographic unit scales. ((a): scatter plot of salinity classes at the national unit scale; (b): Data distribution of salinity levels at the national unit scale; (c): Scatter plot of salinity levels at the comparable geographical unit scale; (d): Data distribution of salinity levels at the comparable geographical unit scale).

The scatter plot (a) and the data distribution graph (b) at the national unit scale show a strong consistency between the salinization intensity map of this study and the excess salts data from HWSD, with a high R^2 value of 0.95. However, due to the disparate areas between countries, the distribution of salinization total levels is highly concentrated, with a majority falling below 1000. From the scatter plot of salinization total levels at the comparable geographical unit scale, it can be observed that there is good consistency between the salinization intensity map of this study and the excess salts data from HWSD, with an R^2 value of 0.86. According to the data distribution graph of salinization total levels at the comparable geographical unit scale, the salinization levels of this study are slightly higher overall compared to those of HWSD's "Excess salts".

4.1.3. Compared to the Salinization Data from GLASOD

The Cs index in the World map of the status of human-induced soil degradation, created by GLASOD, is used to measure the degree of salinization. To compare the results of this study with the salinization data from GLASOD, we conducted a non-parametric correlation test, specifically the Spearman's rank correlation test, at the national and comparable geographical unit scales [60]. The results showed a significant correlation between the two at the 0.01 level. Additionally, the comparison results between the national and comparable geographical units were depicted as scatter plots and data distribution graphs for salinization levels (Figure 7).

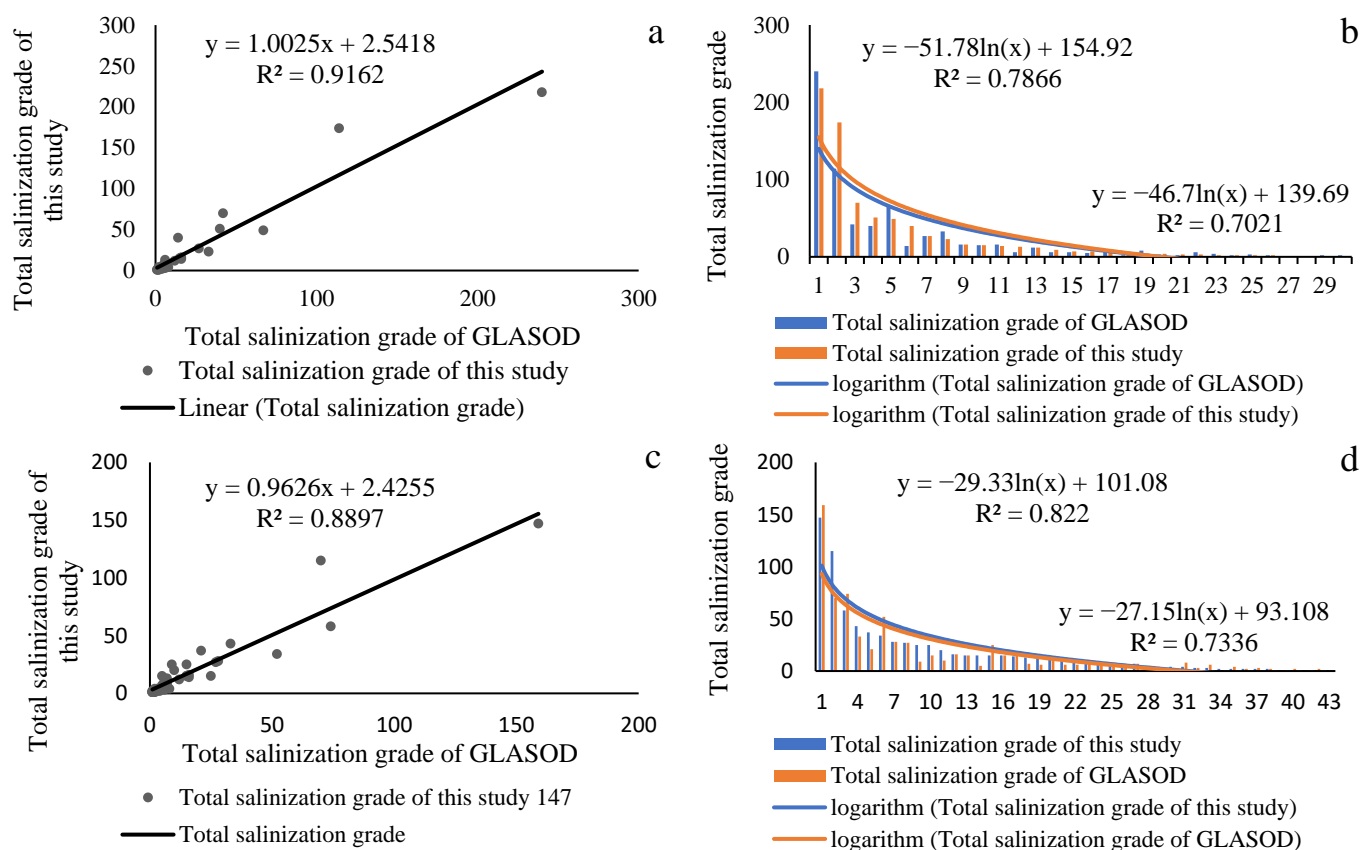


Figure 7. Comparison with GLASOD at national unit and comparable geographic unit scales. ((a): scatter plot of salinity classes at the national unit scale; (b): Data distribution of salinity levels at the national unit scale; (c): Scatter plot of salinity levels at the comparable geographical unit scale; (d): Data distribution of salinity levels at the comparable geographical unit scale).

Although there are not many studies that have the same research scope as this study and GLASOD at the national and comparable geographical unit scales, they still have a strong comparability. As shown in Figure 7, this study and GLASOD had high consistency in their research results at the national unit scale, with an R^2 of up to 0.92. The consistency at the comparable geographical unit scale was slightly lower, with an R^2 of 0.89. Overall, both at the national unit scale and the comparable geographical unit scale, the salinization intensity in this study is slightly higher than the salinization grade in GLASOD.

4.2. Research Value and Policy Recommendations

Salinization significantly affects crop yields, particularly for irrigated crops. Examining the risk of salinization as a hazard can provide vital information for mitigating agricultural losses caused by salinization and promoting sustainable agricultural development. This study utilized salt stress as an indicator to assess hazardous factors, surpassing the limitations associated with using external environmental conditions to establish hazard indicators. The EPIC0509 model was employed to simulate the growth of corn, obtaining results on the global distribution and quantification of corn salinization intensity. This research has made valuable contributions to quantifying regional land degradation and addressing the gap in global salinity risk assessment mapping.

The risk assessment of corn salinization hazard factors under different return periods was conducted based on the principle of information diffusion. This paper introduces a novel approach to studying hazard factors of large-scale salinization, which sets the groundwork for salinization risk assessment. Using salt stress as an indicator for assessing the risk of salinization hazard factors may offer a potential direction for future research. It

serves as a warning against irrational land cultivation practices and the use of transitional groundwater irrigation in ecological transition zones.

Based on the findings of this study, we propose the following recommendations:

- (1) Adapt to climate change by adjusting agricultural production structure and selecting crop varieties with strong resilience to climate impacts.
- (2) Optimize land use and resource allocation by planning agricultural layout based on differences in land productivity potential, improving resource efficiency, and enhancing land protection and improvement measures to prevent salinization.
- (3) Promote carbon-neutral agriculture by reducing greenhouse gas emissions from farming, promoting low-carbon agricultural technologies such as organic farming and precision fertilization, and increasing farmland carbon sequestration through afforestation and wetland conservation.
- (4) Strengthen salinization prevention and control efforts by enhancing monitoring and assessment, developing scientific prevention and control measures such as rational irrigation, drainage infrastructure construction, and soil improvement, and providing training and technical guidance to farmers to enhance their ability to cope with salinization.

4.3. The Outlook and Shortcomings

While this study introduces a new approach to assessing the risk of salinization factors, it overlooks the evaluation of salinization risk in conjunction with corn yield loss rates. The salinization scenario in this study only considers salt stress while disregarding the impact of temperature, precipitation stress, and other forms of land degradation. Additionally, the optimal scenario is applied to all other stress factors without considering their relationship with salinization. In future studies, the following steps will be taken: (1) Integrate disaster risk and production loss rates to construct a global corn salinization vulnerability curve and evaluate the risk of corn salinization worldwide. (2) Further examine the relationship between salinization, temperature stress, and precipitation stress. (3) Investigate the connection between salinization and other forms of land degradation, such as soil erosion and desertification, to achieve a comprehensive evaluation of land degradation. These efforts aim to provide a more comprehensive assessment of salinization and its impact on land degradation.

5. Conclusions

In this study, the salinization hazard factor was determined by the salt stress value. The global cornfield served as the research area, and salinization scenarios were established by eliminating environmental stress factors. Using the EPIC model, the day-step-length salt stress value during the corn growth process was simulated. The risk of corn salinization intensity was evaluated on a global scale, and the intensity of salinization under different return periods was calculated based on the principle of information diffusion. The main conclusions are as follows: (1) Environmental stress factors were eliminated, salinization scenarios were established, and algorithms for the growth season salinization index and disaster intensity index were proposed. (2) High-risk areas (with disruption index > 0.8) for corn salinization were primarily located in Central Asia, northwestern China, southern South America, and the southern coast of Africa. Hazard factors in arid and semi-arid regions posed a high risk, while wet areas had relatively lower risk. (3) The risk of salinization hazard increased with longer return periods (i.e., 10, 20, 50, and 100 years). The impact scope expanded, and the level of danger increased. Oman, Egypt, and Mongolia had an average salinization intensity greater than 0.7, ranking as the top three countries for all return periods. (4) The salinization intensity map produced in this study exhibited high consistency with the Excess salts of HWSD and Cs of GLASOD. The R^2 values between the two results at the country and regional units exceeded 0.9, while the R^2 values at the comparable geographic unit exceeded 0.8. However, the salinization grades in this study were slightly higher overall than those of excess salts of HWSD and Cs of GLASOD.

Author Contributions: Conceptualization, D.L. and F.L.; methodology, D.L. and F.L.; software, D.L.; validation, C.H. and Y.Y.; formal analysis, D.L. and C.H.; investigation, F.L., C.H. and X.G.; resources, J.W.; data curation, D.L. and F.L.; writing—original draft preparation, C.H. and D.L.; writing—review and editing, C.H. and D.L.; visualization, C.H.; supervision, J.W.; project administration, D.L. and J.W.; funding acquisition, J.W. All authors have read and agreed to the published version of the manuscript.

Funding: This study was funded by the 2023 National Social Science Foundation of China (NSSFC) Annual Program (23BSH006), and the Natural Science Foundation of Zhejiang Province, China (LQ21D010009), Wenzhou Philosophy and Social Science Planning Project (No. 22wsk033), and the National Natural Science Foundation of China (Project No. 41271286).

Data Availability Statement: The data used to support the findings of this study can be made available by the corresponding author upon request.

Conflicts of Interest: The authors declare no conflict of interest.

References

1. Wu, W.B.; Verburg, P.H.; Tang, H.J. Understanding land system dynamics and its consequences. *J. Geogr. Sci.* **2018**, *28*, 1563–1566. [CrossRef]
2. Shi, P.J.; Song, C.Q.; Cheng, C.X. Geographical synergetics: From understanding human-environment relationship to designing human-environment synergy. *Acta Geographica Sin.* **2019**, *74*, 3–15.
3. FAO. *Learning about Soil Salinization*; Food and Agriculture Organization: Rome, Italy, 2020.
4. Martinez-Beltran, J. Overview of Salinity Problems in the World and FAO Strategies to Address the Problem. In *Managing Saline Soils and Water: Science, Technology and Social Issues*; Proceedings of the International Salinity Forum; Water Science and Policy Center: Riverside, CA, USA; p. 2005.
5. Davidson, R.A.; Lambert, K.B. Comparing the Hurricane Disaster Risk of U.S. Coastal Counties. *Nat. Hazards Rev.* **2001**, *2*, 132–142. [CrossRef]
6. Huang, J.; Prochazka, M.J.; Triantafyllis, J. Irrigation salinity hazard assessment and risk mapping in the lower Macintyre Valley, Australia. *Sci. Total Environ.* **2016**, *551*, 460–473. [CrossRef] [PubMed]
7. Stofberg, S.F.; Essink, G.H.O.; Pauw, P.S.; De Louw, P.G.; Leijnse, A.; van der Zee, S.E. Fresh water lens persistence and root zone salinization hazard under temperate climate. *Water Resour. Manag.* **2017**, *31*, 689–702. [CrossRef]
8. Bessaim, M.M.; Missoum, H.; Bendani, K.; Bekkouche, M.S. Mitigation of Salinity Hazard from Low Permeable Soil by Electrochemical Treatment: A Laboratory Based Investigation. In *Recent Advances in Geo-Environmental Engineering, Geomechanics and Geotechnics, and Geohazards*; Springer: Berlin/Heidelberg, Germany, 2019; pp. 93–95. [CrossRef]
9. Lobell, D.; Lesch, S.; Corwin, D.; Ulmer, M.; Anderson, K.; Potts, D.; Doolittle, J.; Matos, M.; Baltes, M. Regional-scale assessment of soil salinity in the Red River Valley using multi-year MODIS EVI and NDVI. *J. Environ. Qual.* **2010**, *39*, 35–41. [CrossRef]
10. Furby, S.; Caccetta, P.; Wallace, J. Salinity monitoring in Western Australia using remotely sensed and other spatial data. *J. Environ. Qual.* **2010**, *39*, 16–25. [CrossRef] [PubMed]
11. Caccetta, P.; Dunne, R.; George, R.; McFarlane, D. A methodology to estimate the future extent of dryland salinity in the southwest of Western Australia. *J. Environ. Qual.* **2010**, *39*, 26–34. [CrossRef]
12. Spies, B.; Woodgate, P. *Salinity Mapping Methods in the Australian Context*; Department of the Environment and Heritage: Canberra, Australia, 2005; pp. 23–24.
13. Metternicht, G.I.; Zinck, J. Remote sensing of soil salinity: Potentials and constraints. *Remote Sens. Environ.* **2003**, *85*, 1–20. [CrossRef]
14. De Paz, J.; Visconti, F.; Zapata, R.; Sánchez, J. Integration of two simple models in a geographical information system to evaluate salinization risk in irrigated land of the Valencian Community, Spain. *Soil Use Manag.* **2004**, *20*, 333–342. [CrossRef]
15. Amezketa, E. An integrated methodology for assessing soil salinization, a pre-condition for land desertification. *J. Arid. Environ.* **2006**, *67*, 594–606. [CrossRef]
16. Bouksila, F.; Bahri, A.; Berndtsson, R.; Persson, M.; Rozema, J.; Van der Zee, S.E. Assessment of soil salinization risks under irrigation with brackish water in semiarid Tunisia. *Environ. Exp. Bot.* **2013**, *92*, 176–185. [CrossRef]
17. Rengasamy, P. World salinization with emphasis on Australia. *J. Exp. Bot.* **2006**, *57*, 1017–1023. [CrossRef] [PubMed]
18. Richards, L.A. *Diagnosis and Improvement of Saline and Alkali Soils*; US Government Printing Office: Washington, DC, USA, 1954; Volume 78, p. 154.
19. Sentis, I. Soil Salinization and Land Desertification. *Soil Degrad. Desertif. Mediterr. Environ.* 1996, pp. 105–129. Available online: <https://indico.ictp.it/event/a0114/material/2/14.pdf> (accessed on 10 September 2023).
20. Castrignanò, A.; Buttafuoco, G.; Puddu, R. Multi-Scale Assessment of the Risk of Soil Salinization in an Area of South-Eastern Sardinia (Italy). *Precis. Agric.* **2008**, *9*, 17–31. Available online: <https://link.springer.com/content/pdf/10.1007/s11119-008-9054-4.pdf> (accessed on 10 September 2023). [CrossRef]
21. Mirlas, V. Assessing soil salinity hazard in cultivated areas using MODFLOW model and GIS tools: A case study from the Jezre'el Valley, Israel. *Agric. Water Manag.* **2012**, *109*, 144–154. [CrossRef]

22. Datta, K.; Sharma, V.; Sharma, D. Estimation of a production function for wheat under saline conditions. *Agric. Water Manag.* **1998**, *36*, 85–94. [[CrossRef](#)]
23. Bui, E.N.; Smettem, K.R.; Moran, C.J.; Williams, J. Use of soil survey information to assess regional salinization risk using geographical information systems. *J. Environ. Qual.* **1996**, *25*, 433–439. [[CrossRef](#)]
24. Šimůnek, J.; Suarez, D.L. Two-dimensional transport model for variably saturated porous media with major chemistry. *Water Resour. Res.* **1994**, *30*, 1115–1133. [[CrossRef](#)]
25. Ragab, R. An integrated modelling approach for irrigation water management using saline and non-saline water: The SALTMED model. In Proceedings of the International Symposium on Techniques to Control Salination for Horticultural Productivity, Antalya, Turkey, 7–10 November 2000; Volume 573, pp. 129–138.
26. Raes, D.; Van Goidsenhoven, B.; Goris, K.; Samain, B.; De Pauw, E.; El Baba, M.; Tubail, K.; Ismael, J.; De Nys, E. BUDGET, a management tool for assessing salt accumulation in the root zone under irrigation. In Proceedings of the Inter Regional Conference on Environment-Water, ICID, Fortaleza, Brazil, 27–30 August 2001.
27. Rubio, J.; Calvo, A. *Soil Degradation and Desertification in Mediterranean Environments*; Geofoma Ediciones: Logrono, Barcelona, 1996.
28. Arunrat, N.; Pumijumngong, N.; Hatano, R. Predicting local scale impact of climate change on rice yield and soil organic carbon sequestration: A case study in Roi Et Province, Northeast Thailand. *Agric. Syst.* **2018**, *164*, 58–70. [[CrossRef](#)]
29. FAO. Global Map of Salt-Affected Soils. Available online: <https://www.fao.org/3/cb7247en/cb7247en.pdf> (accessed on 10 September 2023).
30. Kaya, F.; Schillaci, C.; Keshavarzi, A.; Başıyığıt, L. Predictive Mapping of Electrical Conductivity and Assessment of Soil Salinity in a Western Türkiye Alluvial Plain. *Land* **2022**, *11*, 2148. [[CrossRef](#)]
31. Shiferaw, B.; Prasanna, B.M.; Hellin, J.; Bänziger, M. Crops that feed the world 6. Past successes and future challenges to the role played by maize in global food security. *Food Secur.* **2011**, *3*, 307–327. [[CrossRef](#)]
32. Yang, R.; Cao, R.; Gong, X.; Feng, J. Cultivation has selected for a wider niche and large range shifts in maize. *PeerJ* **2022**, *10*, e14019. [[CrossRef](#)] [[PubMed](#)]
33. Farooq, M.; Hussain, M.; Wakeel, A.; Siddique, K.H. Salt stress in maize: Effects, resistance mechanisms, and management: A review. *Agron. Sustain. Dev.* **2015**, *35*, 461–481. [[CrossRef](#)]
34. Williams, J.R.; Wang, E.; Meinardus, A.; Harman, W.; Siemers, M.; Atwood, J.D. *EPIC Users Guide V. 0509*; Blackland Research and Extension Center: Temple, TX, USA, 2006.
35. Williams, J.R. *EPIC: The Erosion-Productivity Impact Calculator*; United States Department of Agriculture: Washington, DC, USA, 1989.
36. Singh, V.P.; Woolhiser, D.A. Mathematical modeling of watershed hydrology. *J. Hydrol. Eng.* **2002**, *7*, 270–292. [[CrossRef](#)]
37. Gassman, P.W.; Reyes, M.R.; Green, C.H.; Arnold, J.G. SWAT peer-reviewed literature: A review. In Proceedings of the 3rd International SWAT Conference, Zurich, Switzerland, 11–15 July 2005. Available online: https://swat.tamu.edu/docs/swat/conferences/2005/PDF/Session_I/Gassman.pdf (accessed on 10 September 2023).
38. Huang, C.F. *Optimality Processing to the Sample Knowledge of Non-Completeness*; Department of Mathematics, Beijing Normal University: Beijing, China, 1992; Volume 28, pp. 129–148.
39. National Soil Erosion-Soil Productivity Research Planning Committee. Soil erosion effects on soil productivity: A research perspective. *J. Soil Water Conserv.* **1981**, *36*, 82–90.
40. Williams, J.R. The erosion-productivity impact calculator (EPIC) model: A case history. *Philos. Trans. R. Soc. Lond. Ser. B Biol. Sci.* **1990**, *329*, 421–428.
41. Williams, J.R.; Jones, C.A.; Dyke, P.T. A modeling approach to determining the relationship between erosion and soil productivity. *Trans. ASAE* **1984**, *27*, 129–144. [[CrossRef](#)]
42. Williams, J.R.; Jones, C.A.; Kiniry, J.R.; Spanel, D.A. The EPIC crop growth model. *Trans. ASAE* **1989**, *32*, 497–511. [[CrossRef](#)]
43. Williams, J.; Nearing, M.; Nicks, A.; Skidmore, E.; Valentin, C.; King, K.; Savabi, R. Using soil erosion models for global change studies. *J. Soil Water Conserv.* **1996**, *51*, 381–385.
44. Stockle, C.O.; Williams, J.R.; Rosenberg, N.J.; Jones, C.A. A method for estimating the direct and climatic effects of rising atmospheric carbon dioxide on growth and yield of crops: Part I—Modification of the EPIC model for climate change analysis. *Agric. Syst.* **1992**, *38*, 225–238. [[CrossRef](#)]
45. Zhi-Qiang, W.; Wei-Hua, F.; Fei, H.E.; Hong, X.U. Effect of climate change on wheat yield in northern China: A research based on EPIC model. *J. Nat. Disasters* **2008**, *17*, 109–114.
46. Anderson, C.J.; Babcock, B.A.; Peng, Y.; Gassman, P.W.; Campbell, T.D. Placing bounds on extreme temperature response of maize. *Environ. Res. Lett.* **2015**, *10*, 124001. [[CrossRef](#)]
47. Bao, Y.; Hoogenboom, G.; McClendon, R.; Vellidis, G. A comparison of the performance of the CSM-CERES-Maize and EPIC models using maize variety trial data. *Agric. Syst.* **2017**, *150*, 109–119. [[CrossRef](#)]
48. Maas, E.V.; Hoffman, G.J.; Chaba, G.D.; Poss, J.A.; Shannon, M.C. Salt sensitivity of corn at various growth stages. *Irrig. Sci.* **1983**, *4*, 45–57. [[CrossRef](#)]
49. Brugnoli, E.; Björkman, O. Growth of cotton under continuous salinity stress: Influence on allocation pattern, stomatal and non-stomatal components of photosynthesis and dissipation of excess light energy. *Planta* **1992**, *187*, 335–347. [[CrossRef](#)] [[PubMed](#)]

50. Pessarakli, M.; Huber, J.; Tucker, T. Dry matter yield, nitrogen absorption, and water uptake by sweet corn under salt stress. *J. Plant Nutr.* **1989**, *12*, 279–290. [[CrossRef](#)]
51. BLISS, R.D.; Platt-Aloia, K.; Thomson, W. Changes in plasmalemma organization in cowpea radicle during imbibition in water and NaCl solutions. *Plant Cell Environ.* **1984**, *7*, 601–606. [[CrossRef](#)]
52. Lauchli, A.; Schubert, S. The Role of Calcium in the Regulation of Membrane and Cellular Growth Processes under Salt Stress. In *Environmental Stress in Plants*; Springer: Berlin/Heidelberg, Germany, 1989; pp. 131–138.
53. Lynch, J.; Cramer, G.R.; Läuchli, A. Salinity reduces membrane-associated calcium in corn root protoplasts. *Plant Physiol.* **1987**, *83*, 390–394. [[CrossRef](#)] [[PubMed](#)]
54. Hichem, H.; El Naceur, A.; Mounir, D. Effects of salt stress on photosynthesis, PSII photochemistry and thermal energy dissipation in leaves of two corn (*Zea mays* L.) varieties. *Photosynthetica* **2009**, *47*, 517–526. [[CrossRef](#)]
55. Cha-Um, S.; Kirdmanee, C. Effect of salt stress on proline accumulation, photosynthetic ability and growth characters in two maize cultivars. *Pak. J. Bot.* **2009**, *41*, 87–98.
56. Khodary, S. Effect of salicylic acid on the growth, photosynthesis and carbohydrate metabolism in salt-stressed maize plants. *Int. J. Agric. Biol.* **2004**, *6*, 5–8.
57. Zhang, Y.F.; Yin, B. Advances in Study of Salt-stress Tolerance in Maize. *J. Maize Sci.* **2008**, *16*, 83–85.
58. Gunes, A.; Inal, A.; Alpaslan, M.; Eraslan, F.; Bagci, E.G.; Cicek, N. Salicylic acid induced changes on some physiological parameters symptomatic for oxidative stress and mineral nutrition in maize (*Zea mays* L.) grown under salinity. *J. Plant Physiol.* **2007**, *164*, 728–736. [[CrossRef](#)] [[PubMed](#)]
59. Volkmar, K.; Hu, Y.; Steppuhn, H. Physiological responses of plants to salinity: A review. *Can. J. Plant Sci.* **1998**, *78*, 19–27. [[CrossRef](#)]
60. Yin, Y.; Zhang, X.; Yu, H.; Lin, D.; Wu, Y.; Wang, J.A. Mapping Drought Risk (Maize) of the World. In *World Atlas of Natural Disaster Risk*; Springer: Berlin/Heidelberg, Germany, 2015; pp. 211–226. [[CrossRef](#)]
61. Huang, C.F.; Liu, X.L.; Zhou, G.X.; Li, X.J. Agricultural natural disaster risk assessment method according to the historic disaster data. *J. Nat. Disasters* **1998**, *7*, 1–9.
62. Miliareisis, G.C.; Argialas, D. Segmentation of physiographic features from the global digital elevation model/GTOPO30. *Comput. Geosci.* **1999**, *25*, 715–728. [[CrossRef](#)]
63. IIASA; FAO. *Global Agro-Ecological Zones—Model Documentation (GAEZ V. 3.0)*; International Institute of Applied Systems Analysis: Vienna, Austria; Food and Agricultural Organization: Rome, Italy, 2012. Available online: https://pure.iiasa.ac.at/id/eprint/13290/1/GAEZ_Model_Documentation.pdf (accessed on 1 September 2022).
64. Warszawski, L.; Frieler, K.; Huber, V.; Piontek, F.; Serdeczny, O.; Schewe, J. The inter-sectoral impact model intercomparison project (ISI-MIP): Project framework. *Proc. Natl. Acad. Sci. USA* **2014**, *111*, 3228–3232. [[CrossRef](#)]
65. Vitousek, P.M.; Mooney, H.A.; Lubchenco, J.; Melillo, J.M. Human domination of Earth’s ecosystems. *Science* **1997**, *277*, 494–499. [[CrossRef](#)]
66. Sacks, W.J.; Deryng, D.; Foley, J.A.; Ramankutty, N. Crop planting dates: An analysis of global patterns. *Glob. Ecol. Biogeogr.* **2010**, *19*, 607–620. [[CrossRef](#)]
67. Tan, G.; Shibasaki, R. Global estimation of crop productivity and the impacts of global warming by GIS and EPIC integration. *Ecol. Model.* **2003**, *168*, 357–370. [[CrossRef](#)]
68. Mueller, N.D.; Gerber, J.S.; Johnston, M.; Ray, D.K.; Ramankutty, N.; Foley, J.A. Closing yield gaps through nutrient and water management. *Nature* **2012**, *490*, 254. [[CrossRef](#)] [[PubMed](#)]
69. ESRI; GRID. Map of Aridity. Available online: <https://data.apps.fao.org/catalog/iso/221072ae-2090-48a1-be6f-5a88f061431a> (accessed on 1 September 2022).
70. Portal, F.S. Harmonized World Soil Database. Available online: <https://www.fao.org/soils-portal/soil-survey/soil-maps-and-databases/harmonized-world-soil-database-v12/zh/> (accessed on 1 September 2022).
71. ISRIC. Global Assessment of Human-Induced Soil Degradation (GLASOD). Available online: <https://www.isric.org/projects/global-assessment-human-induced-soil-degradation-glasod> (accessed on 1 September 2022).
72. Zhang, X.; Zhao, W.; Liu, Y.; Fang, X.; Feng, Q. The relationships between grasslands and soil moisture on the Loess Plateau of China: A review. *Catena* **2016**, *145*, 56–67. [[CrossRef](#)]
73. Wang, X.; Wang, S.; Chen, J.; Cui, H.; Wu, Y.; Ravindranath, N.H.; Rahman, A. Simulating potential yields of Chinese super hybrid rice in Bangladesh, India and Myanmar with EPIC model. *Acta Geogr. Sin.* **2018**, *28*, 1020–1036. [[CrossRef](#)]
74. Guo, H.; Wang, R.; Garfin, G.M.; Zhang, A.; Lin, D.; Liang, Q.; Wang, J. Rice drought risk assessment under climate change: Based on physical vulnerability a quantitative assessment method. *Sci. Total Environ.* **2021**, *751*, 141481. [[CrossRef](#)] [[PubMed](#)]
75. Lian, F. Crop Salinity Vulnerability Curve Construction Based on Epic Model—A Case Study of Global Maize. Doctoral Dissertation, Beijing Normal University, Beijing, China, 2016; pp. 24–25.
76. Tanji, K.K.; Kielen, N.C. *Agricultural Drainage Water Management in Arid and Semi-Arid Areas*; FAO: Rome, Italy, 2002.
77. Katerji, N.; Van Hoorn, J.; Hamdy, A.; Mastrorilli, M. Salinity effect on crop development and yield, analysis of salt tolerance according to several classification methods. *Agric. Water Manag.* **2003**, *62*, 37–66. [[CrossRef](#)]
78. Huang, C.F. Information matrix method for risk analysis of natural disaster. *J. Nat. Disasters* **2006**, *15*, 1–10.
79. Schofield, R.V.; Kirkby, M.J. Application of salinization indicators and initial development of potential global soil salinization scenario under climatic change. *Glob. Biogeochem. Cycles* **2003**, *17*, 4–14–13. [[CrossRef](#)]

80. Yin, Y.; Zhang, X.; Lin, D.; Yu, H.; Wang, J.; Shi, P. GEPIC-V-R model: A GIS-based tool for regional crop drought risk assessment. *Agric. Water Manag.* **2014**, *144*, 107–119. [[CrossRef](#)]
81. Guo, H.; Zhang, X.; Lian, F.; Gao, Y.; Lin, D.; Wang, J. Drought Risk Assessment Based on Vulnerability Surfaces: A Case Study of Maize. *Sustainability* **2016**, *8*, 813. [[CrossRef](#)]
82. Zhang, X.; Guo, H.; Wang, R.; Lin, D.; Gao, Y.; Lian, F.; Wang, J. Identification of the Most Sensitive Parameters of Winter Wheat on a Global Scale for Use in the EPIC Model. *Agron. J.* **2017**, *109*, 58–70. [[CrossRef](#)]

Disclaimer/Publisher’s Note: The statements, opinions and data contained in all publications are solely those of the individual author(s) and contributor(s) and not of MDPI and/or the editor(s). MDPI and/or the editor(s) disclaim responsibility for any injury to people or property resulting from any ideas, methods, instructions or products referred to in the content.